Strict and practical bounds through a non-intrusive and goal-oriented error estimation method for linear viscoelasticity problems

Ludovic Chamoin, Pierre Ladevèze

Strict and practical bounds through a non-intrusive and goal-oriented error estimation method for linear viscoelasticity problems

Ludovic Chamoin [a,*], Pierre Ladevèze [a,b]

[a] LMT-Cachan (ENS-Cachan/CNRS/Paris 6 University), 61 Avenue du Président Wilson, 94235 CACHAN Cedex, France
[b] EADS Foundation Chair, Advanced Computational Structural Mechanics, France

In this work, we set up a non-intrusive procedure that yields for strict and high-quality error bounds of quantities of interest in linear viscoelasticity problems solved by means of the finite element method (FEM). The goal-oriented error estimation approach uses the concept of dissipation error and classical duality techniques involving the solution of an adjoint problem. The non-intrusive feature of this approach is achieved by introducing enrichment functions, via a partition of unity, when solving the adjoint problem numerically (handbook techniques), so that the discretization parameters defined for the primal problem can be reused. The resulting local error estimation method is thus highly effective, easy to implement in a finite element code, and it enables to consider discretization error on truly pointwise quantities of interest.

1. Introduction

In the widespread numerical simulations carried out nowadays, a major concern is the control of the quality of the numerical solutions obtained through approximation methods (such as the finite element method, FEM). Given a mathematical model, considered as the reference, such a control can be relevantly achieved by assessing the so-called *discretization error*. Since the 1970s, several effective techniques have been introduced to deal with global discretization error, i.e. error defined over the global domain of interest; pioneering works on the subject can be found in [1–3]. Today, research intensely focuses on goal-oriented error estimation, that is estimation of the discretization error on local quantities which are relevant for design purposes. On this latter topic, the most accomplished works deal with elliptic problems and give reliable local error bounds [4–8]. However, very few works are dedicated to evolution and non-linear problems [9,10]; furthermore these usually provide for bounds which lack reliability as they are not guaranteed or not sharp, which is a serious drawback for robust design. In the framework of linear viscoelasticity problems described through internal variables and solved with the FEM, we presented in [11] an approach that yields for strict and effective error bounds on local quantities. This approach, which illustrates and extends ideas first introduced in [12], uses classical extraction techniques (leading to the solution of an adjoint problem), the concept of dissipation error, and convexity properties. Moreover, it takes history effects into account and may lead to very sharp error bounds provided that the adjoint problem is solved precisely. A simple but intrusive way to reach such an accurate numerical solution to the adjoint problem was also investigated in [11]; it consists of a local refinement of the time/space mesh being used.

In this paper, we go a step further by setting up a non-intrusive procedure to solve the adjoint problem effectively, in the sense that we reuse the discretization parameters (mesh, operators) defined for the reference (or primal) problem [13]. The procedure is based on handbook techniques [14] and consists in introducing enrichment functions, via the partition of unity method (PUM), when solving the adjoint problem with the FEM. The enrichment functions correspond to locally (quasi-)exact solutions to the adjoint problem; they are given analytically or precomputed numerically in a (semi-)infinite domain. As a result, we get strict and high-quality error bounds at reasonable computational cost, without any remeshing, and the goal-oriented error estimation method can then be implemented quite easily in finite element codes. Furthermore, the non-intrusive framework enables to consider truly pointwise quantities of interest in space and time by using as enrichment functions the well known and possibly infinite energy Green functions.

The present paper is organized as follows: after this introduction, we define in Section 2 the reference linear viscoelasticity problem of interest and the notion of dissipation error. In Section 3, we present the basic goal-oriented error estimation method that enables to get strict error bounds on specific quantities of interest. The non-intrusive version of this method, which is the major breakthrough in

* Corresponding author.
E-mail addresses: ludo@lmt.ens-cachan.fr, chamoin@lmt.ens-cachan.fr (L. Chamoin), ladeveze@lmt.ens-cachan.fr (P. Ladevèze).

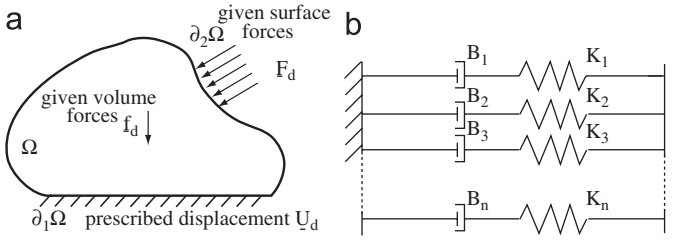

Fig. 1. Structure and its environment (a) and rheological model used (b).

the paper, is described in details in Section 4. Section 5 gives representative results of two-dimensional and three-dimensional numerical experiments. Finally, conclusions are given in Section 6.

2. Reference problem and dissipation error

2.1. Reference problem

Let Ω, with boundary $\partial\Omega$, be an open bounded domain representing a mechanical structure (Fig. 1(a)). This structure is subjected, over the time interval $[0,T]$, to prescribed time-dependent mechanical solicitations. We assume the solicitations can be modeled by a displacement field $\underline{U}_d(M,t)$ on a part $\partial_1\Omega \subset \partial\Omega$, $\partial_1\Omega \neq \emptyset$, a body force field $\underline{f}_d(M,t)$ in Ω, and a traction force density $\underline{F}_d(M,t)$ on the part $\partial_2\Omega$ complementary to $\partial_1\Omega$, such that $\partial_1\Omega \cup \partial_2\Omega = \partial\Omega$ and $\partial_1\Omega \cap \partial_2\Omega = \emptyset$ (Fig. 1(a)).

Under small perturbations assumption, we consider that the behavior of the material can be described by the linear viscoelasticity theory. We choose here the generalized Maxwell model whose rheological model, constituted of an assembly of springs and dashpots, is given in Fig. 1(b). We denote by $\varepsilon(\underline{u})$ the linearized strain tensor, where $\underline{u}(M,t) \in \mathscr{U}^{[0,T]}$ stands for the displacement field in Ω. In each {spring + dashpot} set i, $i = 1,\dots,n$, $\varepsilon(\underline{u})$ can be decomposed into an elastic part ε_i^e and an inelastic part ε_i^p, such that $\varepsilon_i^e + \varepsilon_i^p = \varepsilon(\underline{u})$. We also denote by σ_i the dual variable (in the energy sense) in set i, $i = 1,\dots,n$, such that the Cauchy stress tensor can be defined as

$$\sigma(\underline{u}) = \sum_{i=1}^{n} \sigma_i$$

In the following, previously defined internal variables are represented in a compact form using generalized internal variables (n-vectors):

$$s = \begin{bmatrix} \sigma_1 \\ \cdot \\ \sigma_n \end{bmatrix}, \quad e^e = \begin{bmatrix} \varepsilon_1^e \\ \cdot \\ \varepsilon_n^e \end{bmatrix}, \quad e^p = \begin{bmatrix} \varepsilon_1^p \\ \cdot \\ \varepsilon_n^p \end{bmatrix}, \qquad e = e^e + e^p = \begin{bmatrix} 1 \\ \cdot \\ 1 \end{bmatrix} \varepsilon(\underline{u})$$

Therefore, the intrinsic dissipation reads

$$d = \sum_{i=1}^{n} \mathrm{Tr}[\sigma_i \dot{\varepsilon}_i^p] = s \cdot \dot{e}^p$$

where $\dot{\alpha}$ denotes the time derivative of function α. In the numerical computations, we will choose $n = 3$.

Under quasi-static and isothermal states, the reference problem consists of finding the pair (e^p, s) that verifies

- the compatibility equations:

$$e \in \mathscr{E}^{[0,T]}; \quad e = e^e + e^p; \quad \underline{u}_{|\partial_1\Omega} = \underline{U}_d \quad \forall t \in [0,T] \tag{1}$$

- the balance equations:

$$s \in \mathscr{S}^{[0,T]}; \quad \int_\Omega \mathrm{Tr}[\sigma\varepsilon(\underline{v})]\mathrm{d}\Omega = \int_\Omega \underline{f}_d \cdot \underline{v}\,\mathrm{d}\Omega + \int_{\partial_2\Omega} \underline{F}_d \cdot \underline{v}\,\mathrm{d}S \quad \forall \underline{v} \in \mathscr{V} \quad \forall t \in [0,T] \tag{2}$$

- the initial conditions:

$$e_{p|t=0} = 0 \tag{3}$$

- the constitutive relations, which can be split into two parts:

$$\text{state equations:} \quad e^e = \boldsymbol{\Lambda} s; \quad \sigma = \sum_{i=1}^{n} \sigma_i \tag{4}$$

$$\text{evolution laws:} \quad \dot{e}^p = \boldsymbol{B} s \tag{5}$$

Here, $\mathscr{E}^{[0,T]}$ and $\mathscr{S}^{[0,T]}$ are spaces ensuring enough regularity to get finite energy solutions, and $\mathscr{V}$ is the Banach space of test functions which vanish on $\partial_1\Omega$. Operators $\boldsymbol{\Lambda}$ and $\boldsymbol{B}$ are linear, symmetric, and positive define; $\boldsymbol{\Lambda}$ is provided by classical Hooke's law, whereas $\boldsymbol{B}$ is derived from pseudo-potentials of dissipation.

Remark 1. The reference problem can also be written under a more usual weak form. Find $\underline{u} \in \mathscr{U}^{[0,T]}$ such that

$$B(\underline{u}, \underline{\dot{v}}) = F(\underline{\dot{v}}) \quad \forall \underline{v} \in \mathscr{V}^{[0,T]} \tag{6}$$

where B and F are some bilinear and linear operators, respectively, defined globally over the time–space domain. However, we conserve the definition of the reference problem using (1)–(5) as it points out the evolution laws which are a fundamental concept for the dissipation error which we present in the following.

The exact solution (e_{ex}^p, s_{ex}) of the reference problem is out of reach in practical cases, and we thus resort to numerical methods in order to compute an approximate solution. Practically, we discretize the physical domain Ω using a space mesh $\mathscr{M}_h$, and we split the time domain $[0,T]$ into N time steps of equal length Δt. We then use the FEM associated to a backward-Euler scheme so that we obtain an approximate solution $(e_{h,k}^p, s_{h,k})$ at each time point $t_k = k \times \Delta t$, $k = 0,\dots,N$. Finally, we linearly interpolate over $[0,T]$ the approximate solutions obtained at time points and get an approximate solution (e_h^p, s_h) over $\Omega \times [0,T]$. We define the discretization error on the displacement field as $\underline{\varepsilon}_u = \underline{u}_{ex} - \underline{u}_h$. This error can be measured globally by means of a given norm (such as an energy norm). It can also be specifically defined with respect to quantities of interest, which leads to a local error we will define and assess in Section 3.

2.2. Dissipation error

The concept of dissipation error, introduced in [15], aims at assessing the global discretization error. It requires the possession of a solution $(\hat{e}^p, \hat{s})$, called an admissible solution, that should verify all the equations of the reference problem except the evolution laws (5). Such a solution can be built from the finite element solution (e_h^p, s_h) at hand [11,16]; it is, therefore, denoted by $(\hat{e}_h^p, \hat{s}_h)$ in the following. The numerical construction of $(\hat{e}_h^p, \hat{s}_h)$ merely assumes that the loading $(\underline{U}_d, \underline{f}_d, \underline{F}_d)$ evolves piecewise linearly in time and can be spatially represented by piecewise polynomial functions. Practically, at each time point t_k, $k = 0,\dots,N$:

- We take $\hat{e}_{h,k} = e_{h,k}$ as the (displacement) FEM enables to verify Dirichlet boundary conditions.
- We construct a stress field $\hat{\sigma}_{h,k}$ that verifies the balance Eqs. (2) at $t = t_k$. This major technical point uses properties of $\sigma_{h,k}$ and

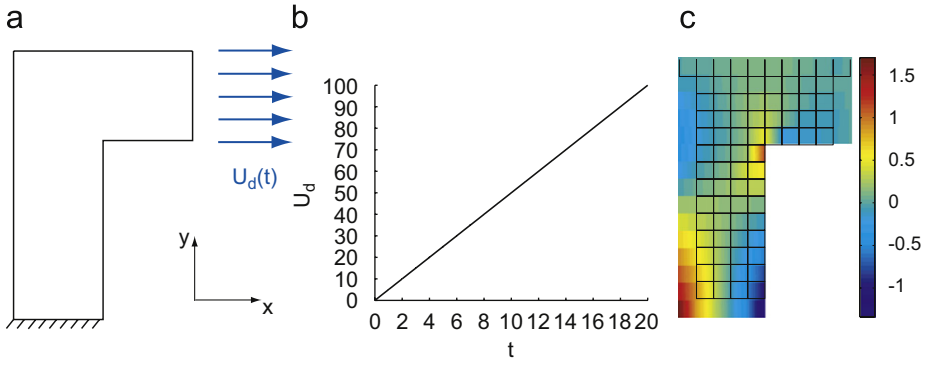

Fig. 2. The reference problem (a), evolution of the loading with time (b), and $\sigma_{h,yy}$ component of the approximate finite element stress field at $t = T$ (c).

requires the solution of local problems over each element of the finite element mesh $\mathscr{M}_h$ [2,16].

- We define a unique solution $\hat{s}_{h,k}$ that minimizes the dissipation error (defined below) over $[t_{k-1}, t_k]$. This step boils down to the solution of constrained minimization problems at Gauss points.
- We compute $\hat{e}^p_{h,k}$ as $\hat{e}^p_{h,k} = \hat{e}_{h,k} - \boldsymbol{\Lambda}\hat{s}_{h,k}$.

Finally, the pairs $(\hat{e}^p_{h,k}, \hat{s}_{h,k})$ obtained at points t_k, $k = 0, \ldots, N$, are linearly interpolated over the time steps in order to obtain an admissible solution $(\hat{e}_h, \hat{s}_h)$ defined over $\Omega \times [0, T]$.

The dissipation error is then defined as a global measure of how much the admissible solution $(\hat{e}^p_h, \hat{s}_h)$ fails to verify (5). It reads

$$E^2_{diss}(\hat{e}^p_h, \hat{s}_h) = \frac{1}{2}\int_0^T \int_\Omega a(t)(\dot{\hat{e}}^p_h - \boldsymbol{B}\dot{\hat{s}}_h)\cdot \boldsymbol{B}^{-1}(\dot{\hat{e}}^p_h - \boldsymbol{B}\dot{\hat{s}}_h)\,\mathrm{d}\Omega\,\mathrm{d}t \geqslant 0 \qquad (7)$$

The time function $a(t)$, positive over $[0, T]$, has been introduced in [11]; it provides a weighted dissipation error, compared to the original definition given in [15,16] and obtained taking $a(t) = 1$. Using a weighted dissipation error enables to take history effects into account, which is a critical aspect for goal-oriented error estimation in evolution problems (see [11] for complete details). The dissipation error is a robust and powerful tool that accounts for all sources of discretization error (time and space discretizations in our case) in nonlinear time-dependent problems. It verifies

$$E_{diss}(\hat{e}^p_h, \hat{s}_h) = 0 \iff (\hat{e}^p_h, \hat{s}_h) = (e^p_{ex}, s_{ex})$$

A fundamental property, which is the true engine to get strict local error bounds, is the relation between $E_{diss}(\hat{e}^p_h, \hat{s}_h)$ and the exact solution (e^p_{ex}, s_{ex}). It is of the form

$$E^2_{diss}(\hat{e}^p_h, \hat{s}_h) = G(s_{ex} - \hat{s}_h) \qquad (8)$$

where G is a given quadratic functional based on free energy and pseudo-potentials of dissipation [11].

We conclude this section with a two-dimensional application of the dissipation error. We consider the structure defined in Fig. 2(a). Its base is clamped and it is subjected to a given time-dependent displacement $\underline{U}_d(t)$ on the top right boundary. The evolution of $\underline{U}_d(t)$ with time is given in Fig. 2(b). A regular space mesh $\mathscr{M}_h$, composed of 100 linear quadrilateral elements with characteristic size h=0.2, is used for the computations. We divide the time interval $[0, T]$ (T=20 s) into 20 time steps. Fig. 2(c) shows the approximate solution obtained at time T using the FEM with a backward-Euler time scheme. After calculating an admissible solution $(\hat{e}^p_h, \hat{s}_h)$, we can compute the corresponding dissipation error $E_{diss}(\hat{e}^p_h, \hat{s}_h)$. The evolution of E_{diss} with respect to the discretization parameters, i.e. the finite element size h and the time step Δt, is given in Fig. 3. We observe that this error tends to zero when both h and Δt become small.

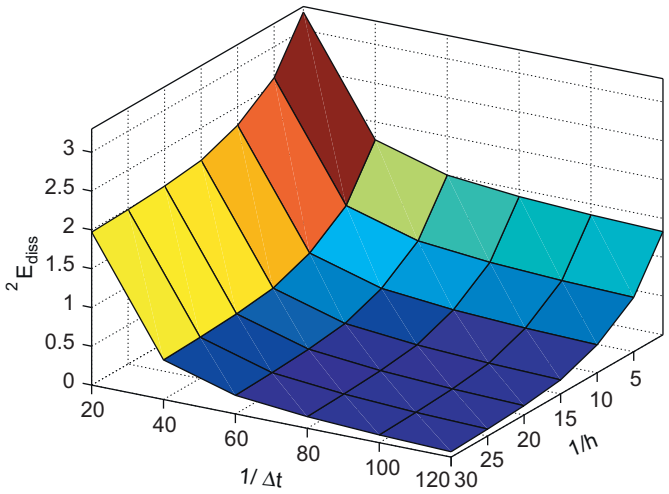

Fig. 3. Evolution of E^2_{diss} with discretization parameters h and Δt.

3. Goal-oriented error estimation

We describe in this section the procedure presented in [11] to get guaranteed bounds of the error on a specified quantity of interest related to the reference linear viscoelasticity problem. The quantity of interest, denoted by I in the following, may be the displacement at a point, the average of a stress component over a local critical region, etc.

3.1. The adjoint problem

We assume that I can be written as a linear functional of the displacement field $\underline{u}$, under the global form

$$I(\underline{u}) = \int_0^T \int_\Omega \sum_{i=1}^n \mathrm{Tr}[\sigma_i(\underline{u})\dot{\tilde{\varepsilon}}_{\Sigma i}]\,\mathrm{d}\Omega\,\mathrm{d}t = \langle\langle s(\underline{u}), \dot{\tilde{e}}_\Sigma\rangle\rangle \qquad (9)$$

where the n-vector $\dot{\tilde{e}}_\Sigma$, known analytically, is called the *extraction function* or *extractor*. Equivalently, we can define by duality the extractor $\tilde{s}_\Sigma$ as $\dot{\tilde{e}}_\Sigma = \boldsymbol{\Lambda}\dot{\tilde{s}}_\Sigma - \boldsymbol{B}\tilde{s}_\Sigma$, $\tilde{s}_{\Sigma|t=T} = 0$, so that

$$I = -\langle\langle \dot{e}(\underline{u}), \tilde{s}_\Sigma\rangle\rangle \qquad (10)$$

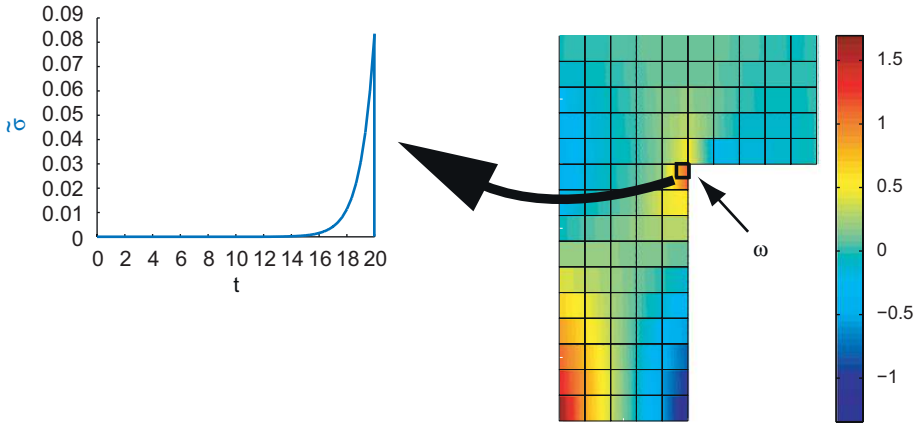

Fig. 4. An example of adjoint problem: the loading is a prescribed time-dependent prestress in a local region $\omega \subset \Omega$.

As an example, we consider the quantity of interest:

$$I = \frac{1}{\omega}\int_{\omega} e^p_{1,yy|t^*}\,\mathrm{d}\Omega \tag{11}$$

that is the mean over a subregion $\omega \subset \Omega$, and at $t = t^*$, of the component $e^p_{1,yy}$ of the internal variable e^p_1. It is straightforward to show that a corresponding extraction function is obtained taking

$$\dot{\tilde{e}}_{\Sigma,1} = \begin{cases} \boldsymbol{B}\begin{bmatrix} 0 & 0 \\ 0 & 1 \end{bmatrix} & \forall\,(M,t) \in \omega \times [0,t^*], \\ \begin{bmatrix} 0 & 0 \\ 0 & 0 \end{bmatrix} & \text{otherwise} \end{cases} \tag{12}$$

the other components of $\dot{\tilde{e}}_{\Sigma}$ being zero.

We aim at assessing the local discretization error:

$$\Delta I = I_{ex} - I_h = I(\underline{u}_{ex}) - I(\underline{u}_h) = I(\underline{u}_{ex} - \underline{u}_h)$$

Following the procedure described in [17], we define $I(\underline{u}_{ex})$ as the result of the constrained minimization problem:

$$I(\underline{u}_{ex}) = \min_{(\underline{u}^*)\in\mathscr{A}} I(\underline{u}^*)$$

where $\mathscr{A} = \{\underline{w} \in \mathscr{U}^{[0,T]}, B(\underline{w},\underline{v}) = F(\underline{v})\ \forall \underline{v} \in \mathscr{V}^{[0,T]}\}$ is the space of displacement fields $\underline{w}^* \in \mathscr{U}^{[0,T]}$ solutions of the reference problem. Using the optimal control theory and searching the saddle-point of the associated Lagrangian:

$$\mathscr{L}(\underline{w},\underline{p}) = I(\underline{w}) - B(\underline{w},\underline{p}) + F(\underline{p}) \qquad \forall (\underline{w},\underline{p}) \in \mathscr{U}^{[0,T]} \times \mathscr{V}^{[0,T]}$$

we derive the following adjoint problem:

Find $(\tilde{e}^p, \tilde{s}) \in \mathscr{E}^{[0,T]} \times \mathscr{S}^{[0,T]}$ that verifies:

- the compatibility equations:

$$\tilde{e} = \tilde{e}^e + \tilde{e}^p\ ;\ \underline{\tilde{u}}_{|\partial_1\Omega} = \underline{0} \quad \forall t \in [0,T]$$

- the balance equations:

$$\int_{\Omega} \mathrm{Tr}[(\tilde{\sigma} - \tilde{\sigma}_{\Sigma})\varepsilon(\underline{v})]\,\mathrm{d}\Omega = 0 \quad \forall \underline{v} \in \mathscr{V},\ \ \forall t \in [0,T]$$

- the final conditions:

$$\tilde{e}_{p|t=T} = 0$$

- the constitutive relations:

$$\text{state equations: } \tilde{e}^e = \boldsymbol{\Lambda}\tilde{s}; \quad \tilde{\sigma} = \sum_{i=1}^{n} \tilde{\sigma}_i \tag{13}$$

$$\text{evolution laws: } \dot{\tilde{e}}^p = -\boldsymbol{B}\tilde{s} \tag{14}$$

This adjoint problem is reverse in time but remains similar to the (primal) reference problem; actually, with the change of variables $\tau = T - t$, the two problems have exactly the same structure. The extractor defined in (10) intervenes in the adjoint problem as a prestress loading.

Remark 2. When considering a quantity of interest I that is directly related to the displacement field (pointwise value of a component of the displacement for instance), the extractor $\tilde{\sigma}_{\Sigma}$ may be defined implicitly. However, the quantity of interest can be in this case defined globally under the form $I = \int_0^T \int_{\Omega} \underline{f}_{\Sigma} \cdot \underline{u}\,\mathrm{d}\Omega\,\mathrm{d}t$, and the loading of the adjoint problem corresponds to a prescribed body force field $\underline{f}_{\Sigma}$.

Using again the two-dimensional example of Fig. 2, and considering the quantity of interest defined in (11) where ω is a local critical region located in the angle and $t^* = T$, the adjoint problem loading consists of a prestress in ω evolving exponentially in time (see Fig. 4).

The corresponding (quasi-) exact stress field $\tilde{\sigma}$ is given in Fig. 5 for $t = T$. It is obtained from a very refined time/space mesh ("overkill solution"). We remark that $\tilde{\sigma}$ presents singularities around the loading region, and that it is very localized (due to St-Venant principle).

3.2. The bounding result

In practice, the exact solution $(\tilde{e}^p_{ex}, \tilde{s}_{ex})$ to the adjoint problem is approximated numerically, with discretization parameters which may be different from those defined to solve the reference problem. We denote by $(\tilde{e}^p_h, \tilde{s}_h)$ the obtained approximate solution. As for the reference problem, we can construct an admissible solution $(\hat{\tilde{e}}^p_h, \hat{\tilde{s}}_h)$ verifying all the equations of the adjoint problem except (14), and compute the corresponding dissipation error:

$$e^2_{diss}(\hat{\tilde{e}}^p_h, \hat{\tilde{s}}_h) = \frac{1}{2}\int_0^T \int_{\Omega} (\dot{\hat{\tilde{e}}}^p_h + \boldsymbol{B}\hat{\tilde{s}}_h) \cdot \boldsymbol{B}^{-1}(\dot{\hat{\tilde{e}}}^p_h + \boldsymbol{B}\hat{\tilde{s}}_h)\,\mathrm{d}\Omega\,\mathrm{d}t \tag{15}$$

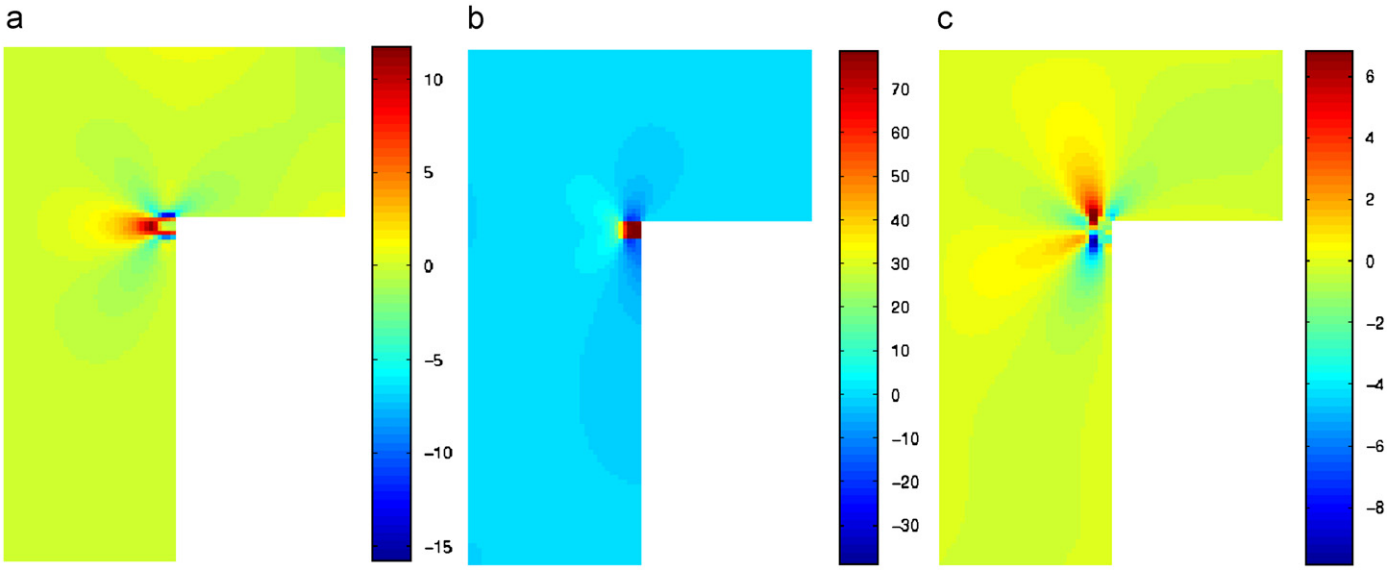

Fig. 5. Quasi-exact solution of the adjoint problem at time T: $\tilde{\sigma}_{xx}$ (a), $\tilde{\sigma}_{yy}$ (b), and $\tilde{\sigma}_{xy}$ (c).

Using duality techniques and the properties of the dissipation error, the following result can be shown (see [11,18] for complete details):

$$\left| I_{ex} - I_h - I_{hh} \right| \leqslant 2\left[\tfrac{1}{2} E^2_{diss}\left(\hat{e}^p_h, \hat{s}_h\right) + F_0(\Delta_h) \right]^{1/2} \cdot \left[F_2(\tilde{x}_h) ig \right]^{1/2} \tag{16}$$

In this expression, I_{hh} is a correction term computable from the approximate solutions of both reference and adjoint problems, F_0 and F_2 are some functions known analytically, Δ_h is a given term that is not explicited here, and $\tilde{x}_h = \dot{\hat{e}}^p_h + \boldsymbol{B}(\hat{s}_h)$. The term $F_2(\tilde{x}_h)$ is very similar to $e^2_{diss}(\hat{e}^p_h, \hat{s}_h)$ and behaves the same way, despite the two expressions are different. We thus obtain from (16) some guaranteed bounds ξ_{inf} and ξ_{sup} of I_{ex}:

$$\begin{aligned} \xi_{inf} &= I_h + I_{hh} - 2[\tfrac{1}{2} E^2_{diss}(\hat{e}^p_h, \hat{s}_h) + F_0(\Delta_h)]^{1/2} . [F_2(\tilde{x}_h)]^{1/2} \\ \xi_{sup} &= I_h + I_{hh} + 2[\tfrac{1}{2} E^2_{diss}(\hat{e}^p_h, \hat{s}_h) + F_0(\Delta_h)]^{1/2} \cdot [F_2(\tilde{x}_h)]^{1/2} \end{aligned} \tag{17}$$

and $I_h + I_{hh}$ can be viewed as a new approximation of I_{ex}. Equivalently, bounds for the local error $I_{ex} - I_h$ can be derived from (16). It is fruitful noticing that the robust local error estimation we obtain requires the solution of a complementary problem and the computation of the two global error estimates $E^2_{diss}(\hat{e}^p_h, \hat{s}_h)$ and $F_2(\tilde{x}_h)$.

Another important remark is that the upper bound in (16) may be reduced by making the term $F_2(\tilde{x}_h)$ small, which is the case when the numerical solution of the adjoint problem is accurate enough. Therefore, from any given approximate solution to the reference problem, bounds ξ_{inf} and ξ_{sup} of the exact unknown value I_{ex} can be very sharp provided that the adjoint problem is solved precisely. Ultimately, when the approximate solution $(\tilde{e}^p_h, \tilde{s}_h)$ converges to the exact solution $(\tilde{e}^p_{ex}, \tilde{s}_{ex})$, $F_2(\tilde{x}_h)$ tends to zero and the correction term I_{hh} tends to $I_{ex} - I_h$. In [11], an accurate solution of the adjoint problem was obtained by refining locally the time/space mesh used to solve the adjoint problem (see Fig. 6 for an example of a locally refined space mesh for the adjoint problem defined in Fig. 4). However, this technique is non-intrusive as it leads to large modifications in a finite element code. Furthermore, it can be prohibitive in cases where a very fine mesh is necessary to obtain an acceptable solution.

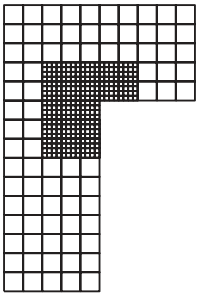

Fig. 6. Locally refined space mesh providing an accurate approximate solution to the adjoint problem. The refinement is performed in subregions of Ω where the dissipation error $e^2_{diss}(\hat{e}^p_h, \hat{s}_h)$ has large contributions.

4. Non-intrusive approach to get sharp local error bounds

4.1. The non-intrusive procedure

We present now a concurrent procedure to solve the adjoint problem with high accuracy. It is inspired from the fact that the solution to the adjoint problem can be divided into two parts: a part with high gradients (in space and time) in localized regions of the domain $[0,T] \times \Omega$, and a smooth part in the remainder of the time-space domain. The former may be difficult to catch by means of a standard FEM and requires high computational costs. However, the singularities due to the loading of the adjoint problem are usually well known as they are directly related to the quantity of interest which is considered and to material parameters. Aiming at introducing the singular part of the solution explicitly when solving the adjoint problem with the FEM, we use a procedure based on the handbook techniques developed in [14]. There are two steps in the procedure:

(1) We first define some enrichment functions which correspond to singular solutions $(\tilde{e}^{hand,p}, \tilde{s}^{hand})$ of the adjoint problem loadings over an infinite (or semi-infinite) domain. They are usually computed analytically in time (using the Laplace transform) and numerically in space, and constitute a library of pre-calculated solutions (examples are given in Figs. 7 and 8).

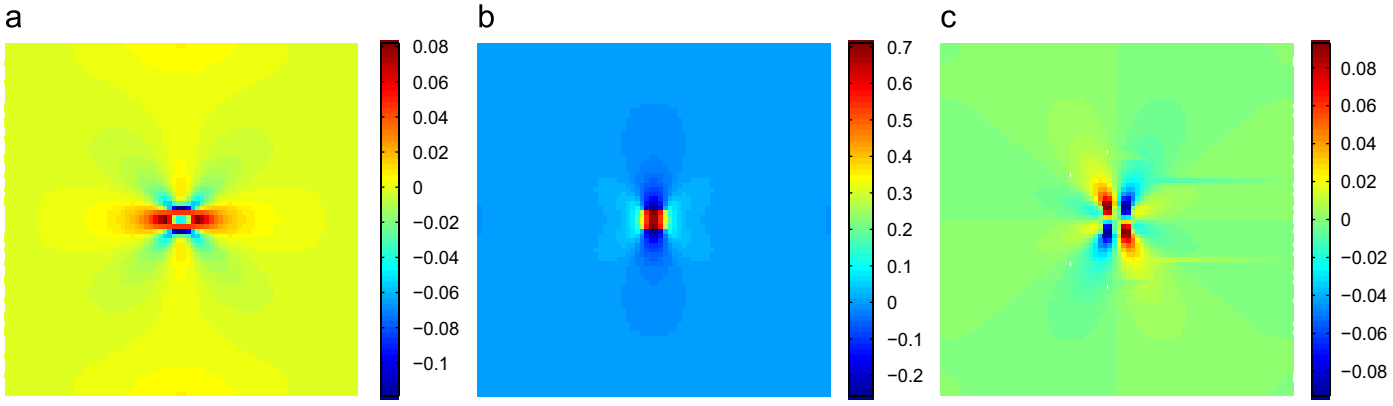

Fig. 7. Evolution in space of the handbook stress field corresponding to a prestress loading $\tilde{\sigma}_\Sigma$ over an infinite domain: $\tilde{\sigma}_{xx}^{hand}$ (a), $\tilde{\sigma}_{yy}^{hand}$ (b), and $\tilde{\sigma}_{xy}^{hand}$ (c).

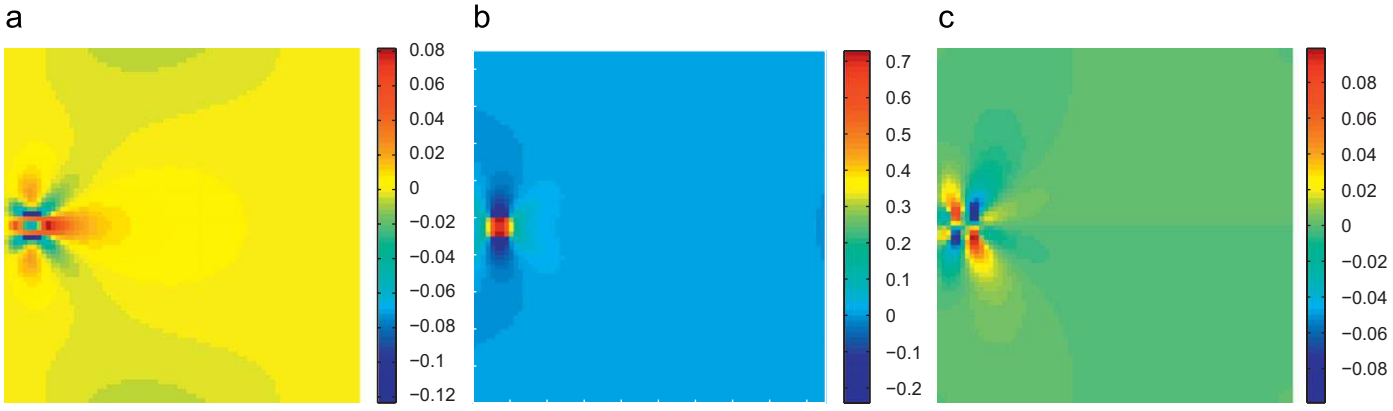

Fig. 8. Evolution in space of the handbook stress field corresponding to a prestress loading $\tilde{\sigma}_\Sigma$ over a semi-infinite domain: $\tilde{\sigma}_{xx}^{hand}$ (a), $\tilde{\sigma}_{yy}^{hand}$ (b), and $\tilde{\sigma}_{xy}^{hand}$ (c).

(2) Secondly, we introduce the adequate enrichment functions, via the PUM, in the set of basis functions describing the approximate displacement field of the adjoint problem.

The expression of the latter displacement field then becomes

$$\underline{\tilde{u}} = \sum_{j \in \mathcal{N}^{PUM}} \psi_j \underline{\tilde{u}}^{hand} + \underline{\tilde{u}}^r \tag{18}$$

where ψ_j is the classical linear finite element shape function associated to node j, $\mathcal{N}^{PUM}$ is the set of nodes in $\mathscr{M}_h$ concerned by the enrichment with the PUM, and $\underline{\tilde{u}}^r$ is a displacement field to be calculated. Let us note that we do not introduce any new degree of freedom in the formulation: the degrees of freedom associated to the PUM are known, i.e. the enrichment is entirely determined, and only the field $\underline{\tilde{u}}^r$ is unknown. The global solution thus reads $(\tilde{e}^p, \tilde{s}) = (\tilde{e}_{PUM}^{hand,p}, \tilde{s}_{PUM}^{hand}) + (\tilde{e}^{r,p}, \tilde{s}^r)$. It is composed of two terms:

(i) an enrichment term $(\tilde{e}_{PUM}^{hand,p}, \tilde{s}_{PUM}^{hand})$ which locally equilibrates the loading of the adjoint problem but does not verify all the boundary conditions on $\partial\Omega$;
(ii) an unknown term $(\tilde{e}^{r,p}, \tilde{s}^r)$which can be seen as a residual solution and that enables to verify all the boundary conditions on $\partial\Omega$.

The new problem we thus have to solve consists in finding the residual solution $(\tilde{e}^{r,p}, \tilde{s}^r)$. It retains the same structure as the original adjoint problem except that the balance equations read

$$\int_\Omega \mathrm{Tr}[\tilde{\sigma}^r \varepsilon(\underline{v})]\,\mathrm{d}\Omega = \int_\Omega \mathrm{Tr}[(\tilde{\sigma}_\Sigma - \tilde{\sigma}_{PUM}^{hand})\varepsilon(\underline{v})]\,\mathrm{d}\Omega \quad \forall \underline{v} \in \mathscr{V},\ \forall t \in [0,T] \tag{19}$$

We denote by Ω^{PUM} the region in Ω which is involved in the enrichment with the PUM; it corresponds to the support of $\sum_{j \in \mathcal{N}^{PUM}} \psi_j$. Ω^{PUM} can be divided into two subregions Ω_1^{PUM} and Ω_2^{PUM}, with $\Omega_1^{PUM} \cup \Omega_2^{PUM} = \Omega^{PUM}$ and $\Omega_1^{PUM} \cap \Omega_2^{PUM} = \emptyset$, Ω_1^{PUM} corresponding to the region where $\sum_{j \in \mathcal{N}^{PUM}} \psi_j = 1$ (see Fig. 9). With these notations,

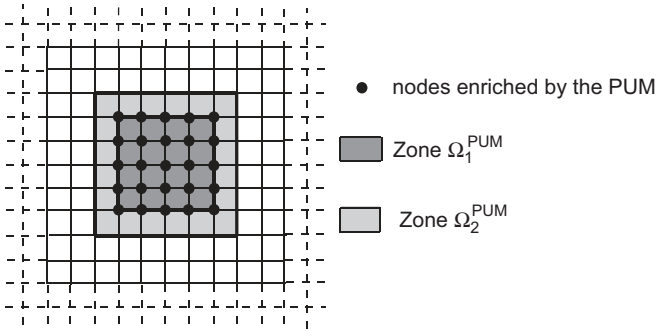

Fig. 9. Definition of zones Ω_1^{PUM} and Ω_2^{PUM}.

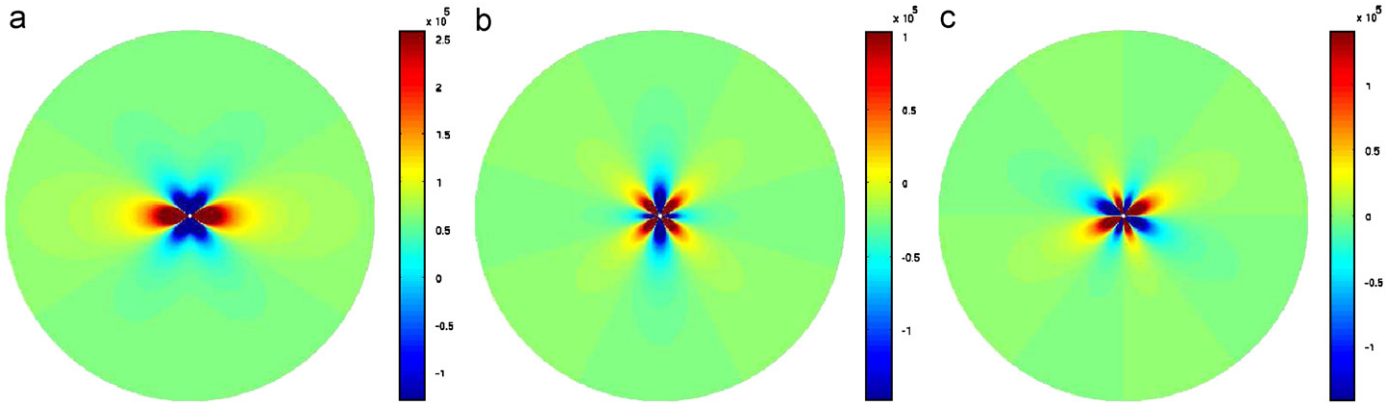

Fig. 10. Spatial distribution of the stress field corresponding to a pointwise prestress loading over a two-dimensional infinite domain: $\tilde{\sigma}_{xx}^{hand}$ (a), $\tilde{\sigma}_{yy}^{hand}$ (b), and $\tilde{\sigma}_{xy}^{hand}$ (c).

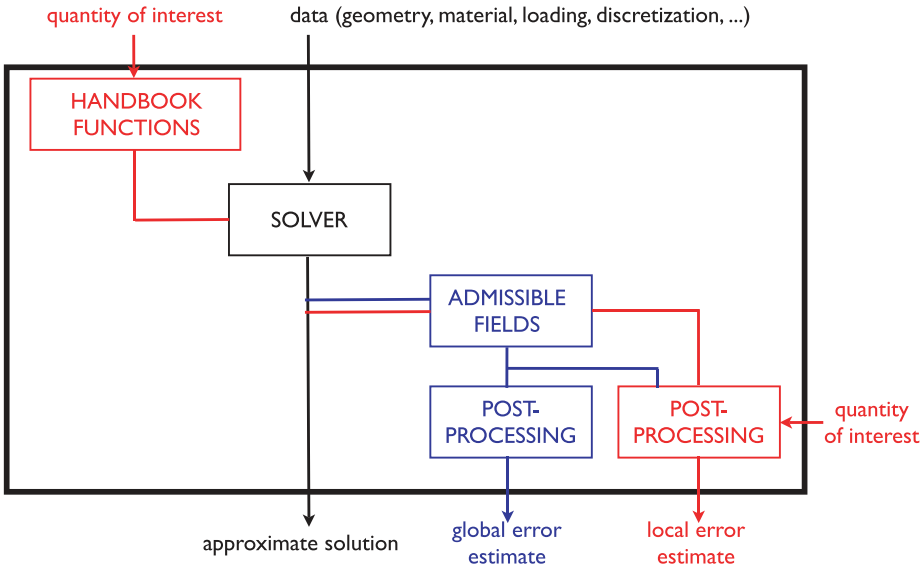

Fig. 11. General implementation of the non-intrusive local error estimation method into a finite element code. Elements corresponding to the basic framework for the finite element computation are given in black; elements corresponding to the postprocessing of the numerical solution with a global error estimation are given in blue; elements corresponding to the goal-oriented error estimation are given in red. (For interpretation of the references to colour in this figure legend, the reader is referred to the web version of this article).

(19) can be recast in the form

$$\int_\Omega \mathrm{Tr}[\tilde{\sigma}^r \varepsilon(\underline{v})]\,\mathrm{d}\Omega = -\int_{\partial\Omega_1^{PUM}} \tilde{\sigma}^{hand}\underline{n}_{12}\cdot\underline{v}\,\mathrm{d}\Omega - \int_{\Omega_2^{PUM}} \mathrm{Tr}[\tilde{\sigma}_{PUM}^{hand}\varepsilon(\underline{v})]\,\mathrm{d}\Omega \quad \forall \underline{v}\in\mathscr{V},\ \forall t\in[0,T] \tag{20}$$

where $\underline{n}_{12}$ is the outgoing normal vector on the boundary $\partial\Omega_1^{PUM}$. Properties of the enrichment function are used to obtain (20).

We observe from (20) that the loading of the new adjoint problem is now smoother, and therefore an accurate approximation $(\tilde{e}_h^{r,p},\tilde{s}_h^r)$ of the residual term $(\tilde{e}^{r,p},\tilde{s}^r)$ can be obtained using the FEM with the same time/space discretization as the one used for the reference problem. The method is called non-intrusive in this sense: we reuse the discretization parameters (space–time mesh, factorized stiffness matrix, etc.) defined for the numerical solution of the reference problem; only the loading vector and Dirichlet boundary conditions have to be changed between the two computations. Practically, reference and adjoint problems are solved in the same time.

Eventually, we get an approximate solution $(\tilde{e}_h^p,\tilde{s}_h)$ of the adjoint problem, such that $(\tilde{e}_h^p,\tilde{s}_h)=(\tilde{e}_{PUM}^{hand,p},\tilde{s}_{PUM}^{hand})+(\tilde{e}_h^{r,p},\tilde{s}_h^r)$. After computing an admissible residual solution $(\hat{\tilde{e}}_h^{r,p},\hat{\tilde{s}}_h^r)$ with classical tools, the bounding result (16) holds with

$$\tilde{x}_h = -\boldsymbol{B}(\hat{\tilde{s}}_h)-\hat{\dot{\tilde{e}}}_h^p = -\boldsymbol{B}(\hat{\tilde{s}}_h^r)-\hat{\dot{\tilde{e}}}_h^{r,p}$$

due to the fact that the evolution laws are verified by the handbook solutions. As regards term I_{hh} involved in (16), which involves the enrichment $(\tilde{e}_{PUM}^{hand,p},\tilde{s}_{PUM}^{hand})$, it is calculated using overintegration.

4.2. Case of pointwise quantities of interest

The extension of the non-intrusive method to pointwise in space quantities of interest is straightforward. Indeed, the associated handbook functions correspond, in that case, to the well known *Green functions* (whereas handbook functions in the general case

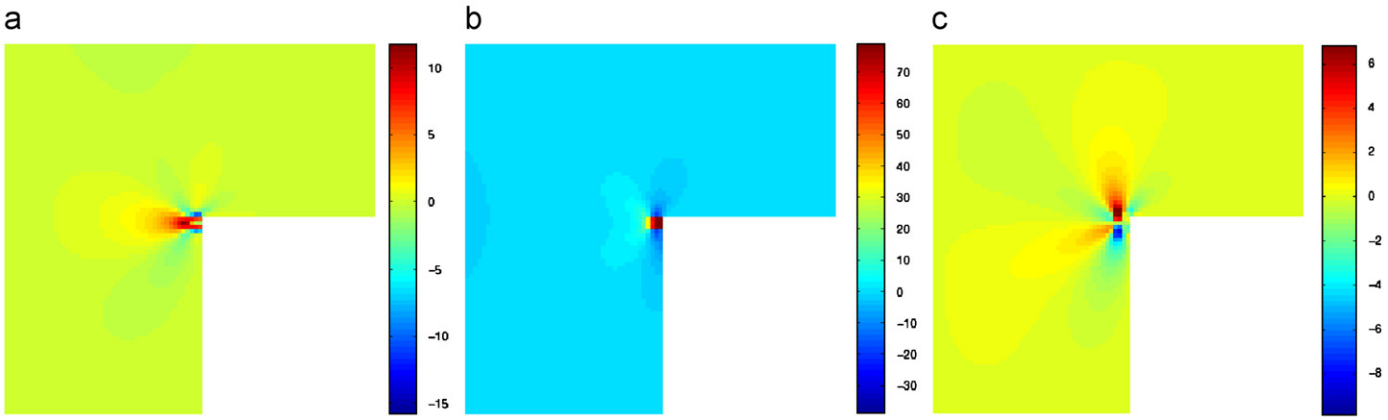

Fig. 12. Evolution in space of the handbook function $\tilde{\sigma}^{hand}$ at time T: $\tilde{\sigma}^{hand}_{xx}$ (a), $\tilde{\sigma}^{hand}_{yy}$ (b), and $\tilde{\sigma}^{hand}_{xy}$ (c).

correspond to the *generalized Green functions*). One can introduce such functions, even though they are usually infinite-energy, into the approximate solution to the adjoint problem as they do not appear in the expression of the upper bound given in (16). The Green functions are here calculated analytically in space and time, using techniques based on strain nuclei and the image method (see [19–21] for details). An example of such a Green function is given in Fig. 10.

However, as the finite element value I_h of a pointwise quantity at some point P within Ω is not always defined (due to possible discontinuities of the derivatives across element boundaries), we recast (16) into the form

$$\left| I_{ex} - \hat{I}_h - \hat{I}_{hh} \right| \leqslant 2\left[\tfrac{1}{2}E^2_{diss}\left(\hat{e}^p_h, \hat{s}_h\right) + F_0(\Delta_h)\right]^{1/2} \cdot \left[F_2(\tilde{x}_h)\right]^{1/2} \qquad (21)$$

where $\hat{I}_h$ and $\hat{I}_{hh}$ are some quantities defined at any regular point P from the admissible solution $(\hat{e}^p_h, \hat{s}_h)$. Therefore, (21) provides some strict and guaranteed bounds of the exact value I_{ex} of a pointwise quantity, such as a component of displacement or stress at a point.

As a conclusion of this section, we given Fig. 11 a diagram illustrating the implementation of the non-intrusive local error estimation method into a finite element code equipped with a global error estimator based on the dissipation error beforehand. We observe that blocks preexisting in the code are reused, and little effort is required to insert the goal-oriented error estimation method (blocks in red).

5. Numerical results

In the following examples, the calculation of I_{ex}, used as the reference value, is performed using a "quasi-exact" solution obtained by means of a very refined finite element mesh ("*overkill solution*"). Practically, the mesh is refined until the approximate value of I_{ex} has converged.

5.1. A two-dimensional example with a quantity of interest defined as an average

We apply the non-intrusive procedure to the adjoint problem defined in Fig. 4. The reference problem is the one given in Fig. 2 and the quantity of interest we consider is

$$I = \frac{1}{\omega}\int_{\omega} e^p_{1,yy|T}\,\mathrm{d}\Omega \qquad (22)$$

Fig. 12 shows the enrichment function which is used to solve the adjoint problem.

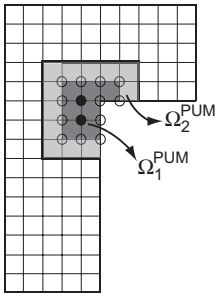

Fig. 13. Enrichment with the PUM and definition of zones Ω_1^{PUM} et Ω_2^{PUM}: enriched nodes are circled.

The enrichment is introduced with the PUM over a subregion of Ω located in the neighborhood of the loading of the adjoint problem (Fig. 13). We therefore obtain solutions $(\tilde{e}^{hand,p}_{PUM}, \tilde{s}^{hand}_{PUM})$, $(\tilde{e}^{r,p}, \tilde{s}^r)$, and $(\tilde{e}^p_h, \tilde{s}_h) = (\tilde{e}^{hand,p}_{PUM}, \tilde{s}^{hand}_{PUM}) + (\tilde{e}^{r,p}, \tilde{s}^r)$ whose corresponding stress fields are given in Figs. 14, 15, and 16, respectively.

We thus obtain the strict bounds:

$$\bar{\xi}_{inf} = \frac{\xi_{inf}}{I_{ex}} = 0.97, \quad \bar{\xi}_{sup} = \frac{\xi_{sup}}{I_{ex}} = 1.02$$

that is an approximation of I_{ex} with a precision higher than 3%.

5.2. A two-dimensional example with a pointwise quantity of interest

We now consider the pointwise quantity of interest

$$I = \dot{\varepsilon}^p_{1_{yy}}(P)_{|T}$$

where P is located in an element close to a traction free boundary of Ω (Fig. 17).

Remark 3. It would be possible to take P inside the critical region ω defined previously. However, as the solution has a singularity in this region, considering a pointwise quantity of interest is not very relevant for design purposes. Taking quantities of interest such as stress intensity factors would make more sense in that case.

The adjoint problem corresponds to a pointwise prestress located at point P and evolving exponentially in time (Fig. 18).

The analytical enrichment function we use, taking traction-free boundary conditions into account, is similar to the one given in

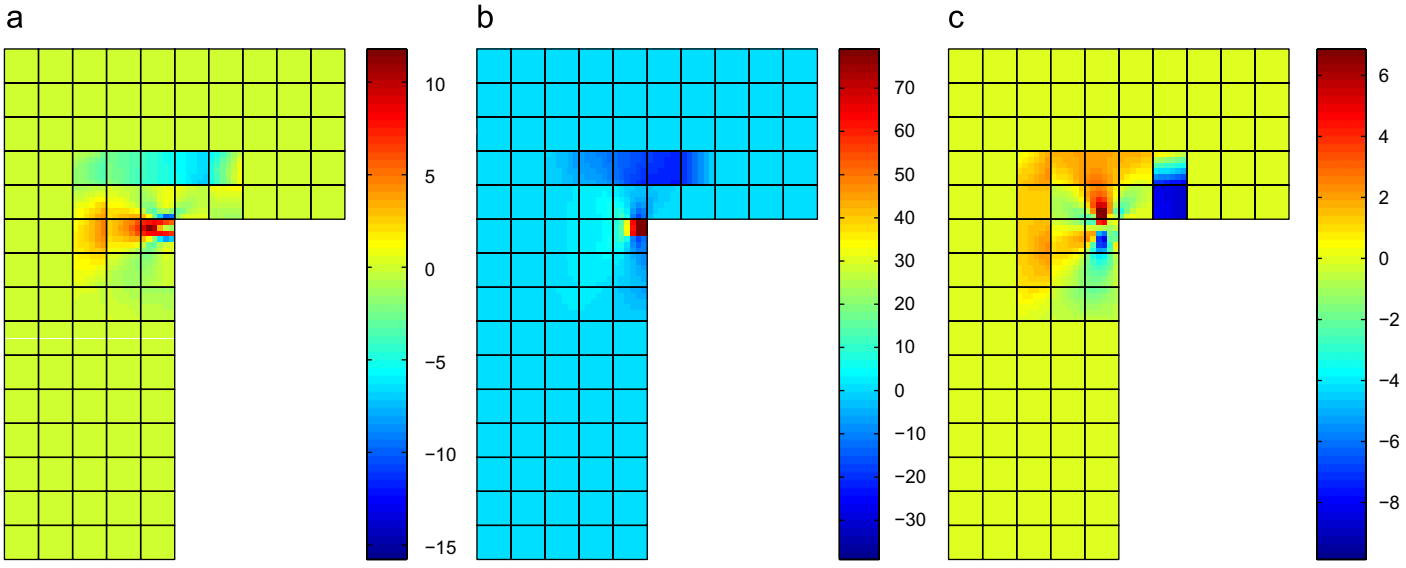

Fig. 14. Evolution in space of the stress field $\tilde{\sigma}^{hand}_{PUM}$ at time T: $\tilde{\sigma}^{hand}_{PUM_{xx}}$ (a), $\tilde{\sigma}^{hand}_{PUM_{yy}}$ (b), and $\tilde{\sigma}^{hand}_{PUM_{xy}}$ (c).

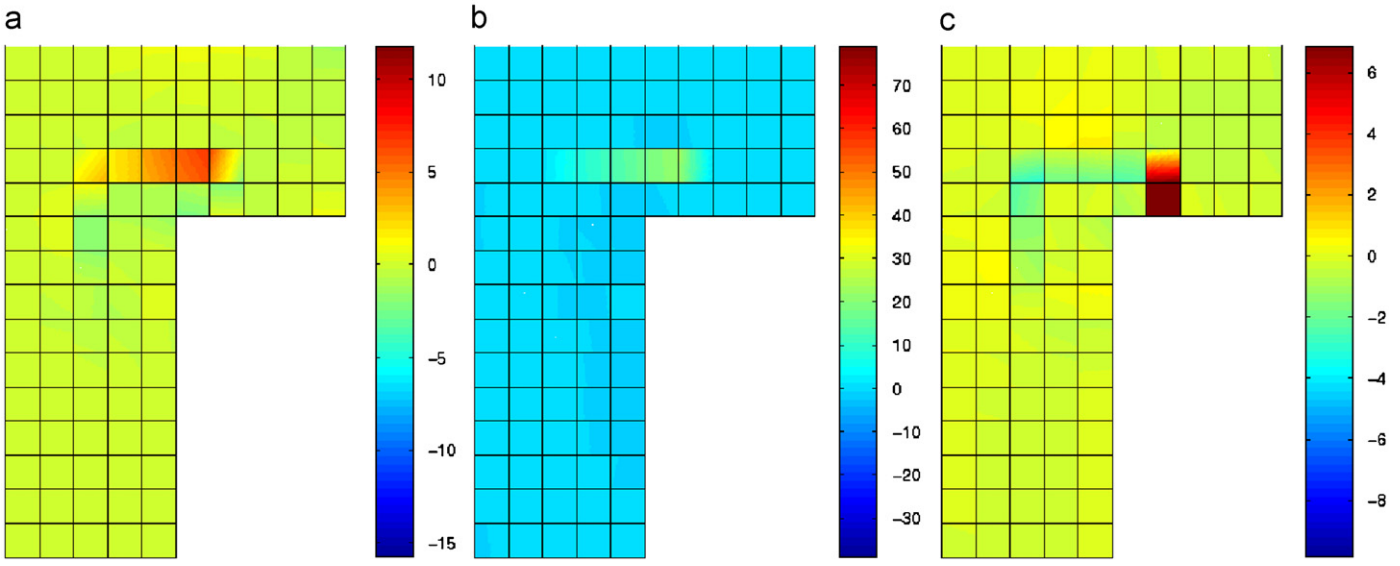

Fig. 15. Evolution in space of the stress field $\tilde{\sigma}^{r}_{h}$ at time T: $\tilde{\sigma}^{r}_{h_{xx}}$ (a), $\tilde{\sigma}^{r}_{h_{yy}}$ (b), and $\tilde{\sigma}^{r}_{h_{xy}}$ (c).

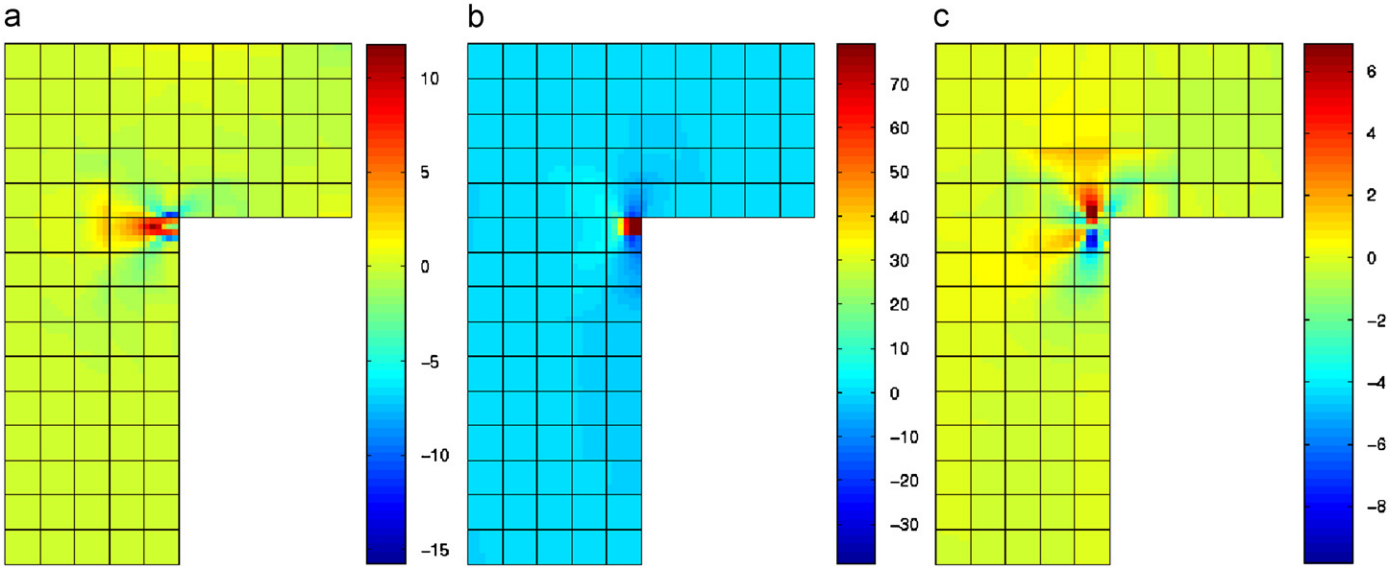

Fig. 16. Evolution in space of the stress field $\tilde{\sigma}_{h}$ at time T: $\tilde{\sigma}_{h_{xx}}$ (a), $\tilde{\sigma}_{h_{yy}}$ (b), and $\tilde{\sigma}_{h_{xy}}$ (c).

Fig. 10; it represents the exact solution of the adjoint problem loading over a semi-infinite domain. The enrichment is introduced in the approximate solution to the adjoint problem through the PUM applied at specific nodes of the mesh i.e. nodes close to point P (these nodes are circled in Fig. 18). We then get the following bounds:

$$\bar{\xi}_{inf} = 0.96, \quad \bar{\xi}_{sup} = 1.04$$

which shows that the non-intrusive method is very effective and enables to obtain accurate bounds of localized quantities through the enrichment of only a few nodes of the space mesh. However, even higher precision could be reached by enlarging the size of Ω^{PUM}, i.e. introducing the enrichment on more nodes.

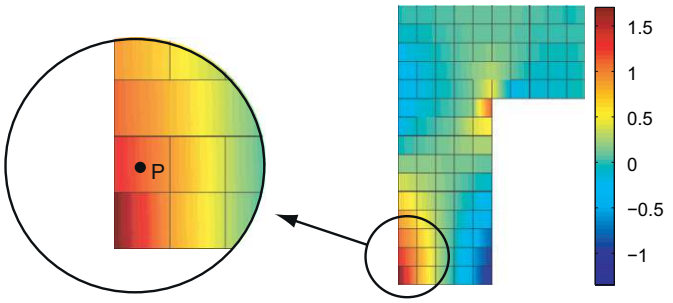

Fig. 17. Definition of the point P where the quantity of interest is defined.

In addition, the non-intrusive local error estimation method enables to seek lower and upper bounds of $I_{ex}(\mathrm{P})$ for any point P within a specific local zone of interest $E \subset \Omega$ (Fig. 19). The procedure consists in sweeping over E, considering that the residual solution $(\tilde{e}_h^{r,p}, \tilde{s}_h^r)$ of the adjoint problem does not depend on the localization of P over E (practically, this is verified if the enrichment zone is sufficiently large). Therefore, only the handbook function has to be changed when sweeping over E, and the following result yields:

$$\left| I_{ex}(\mathrm{P}) - \hat{I}_h(\mathrm{P}) - \hat{I}_{hh}(\mathrm{P}) \right| \leqslant 2\left[\tfrac{1}{2} E^2_{diss}\left(\hat{e}_h^p, \hat{s}_h\right) + F_0(\Delta_h) \right]^{1/2} \cdot [F_2(\tilde{x}_h)]^{1/2}$$
$$\forall P \in E$$

The method provides the following bounds for the extremum $I_{ex}^{max,E}$ of I_{ex} over E:

$$\bar{\xi}^E_{inf} = \frac{\xi^E_{inf}}{I_{ex}^{max,E}} = 0.95, \quad \bar{\xi}^E_{sup} = \frac{\xi^E_{sup}}{I_{ex}^{max,E}} = 1.05$$

As a result, we are able to obtain high-quality lower and upper bounds for the extremum of I_{ex} (or L^∞-norm of I_{ex}) over a given subregion of Ω, which may constitute useful information for analysts/designers.

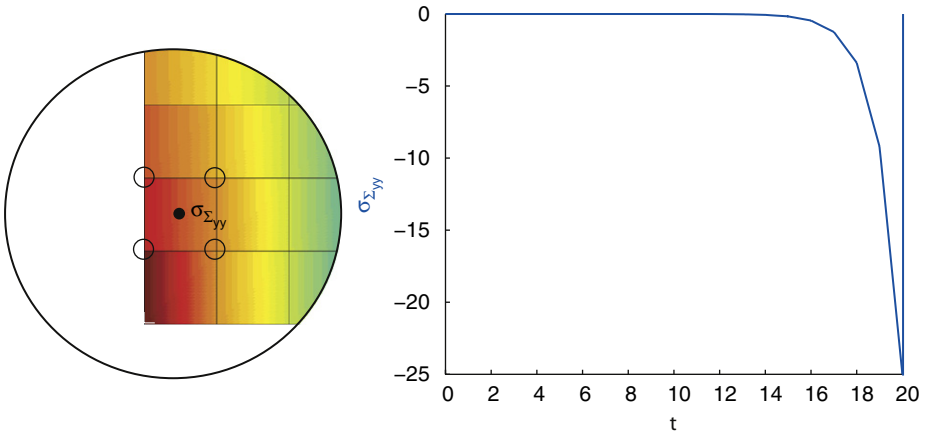

Fig. 18. Definition of the loading for the adjoint problem.

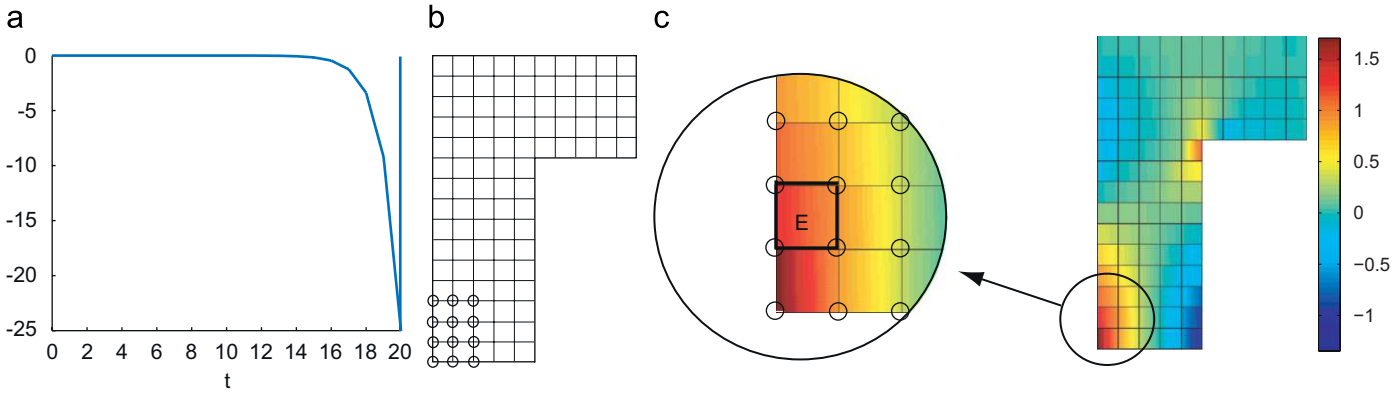

Fig. 19. Evolution of $\tilde{\sigma}_\Sigma$ with respect to time (a), nodes involved in the enrichment through the PUM (b), and definition of zone E (c).

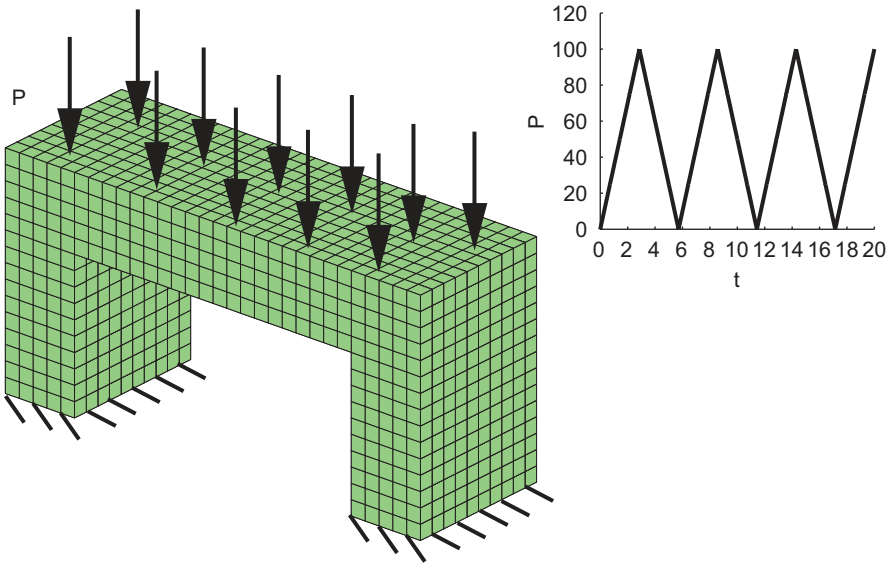

Fig. 20. Definition of the three-dimensional reference problem.

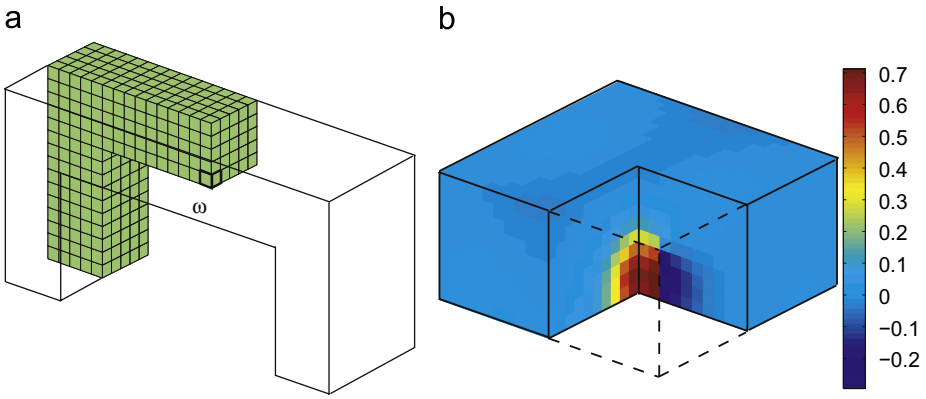

Fig. 21. Definition of the subregion of interest ω (a), and enrichment function used in the non-intrusive procedure (b).

5.3. A three-dimensional example

The last application deals with a three-dimensional structure which is clamped at its base and subjected to a uniform pressure p on its upper face (Fig. 20). Pressure p is imposed with a cyclic evolution in time.

The structure is discretized in space with a regular mesh $\mathscr{M}_h$ made of linear cubic finite elements (10 098 degrees of freedom). We consider the quantity of interest:

$$I = \frac{1}{\omega}\int_{\omega} \sigma_{xx|T}\,\mathrm{d}\Omega$$

where ω corresponds to a finite element defined in a critical region of Ω (Fig. 21).

The enrichment function corresponds to a prestress loading over a semi-infinite domain (see Fig. 21); it is given analytically in time and computed numerically in space. It is introduced in the formulation of the adjoint problem by enriching with the PUM two layers of nodes around zone ω. The non-intrusive goal-oriented error estimation method then provides for the bounds:

$$\bar{\xi}_{inf} = 0.95, \quad \bar{\xi}_{sup} = 1.07$$

6. Conclusion

We presented in this paper a method that gives strict, high-quality, and practical error bounds of local quantities in linear viscoelasticity problems. It is made non-intrusive due to the fact that by using handbook techniques, the adjoint problem is solved precisely while keeping unchanged the discretization parameters and operators defined for the reference problem; only the loading and boundary conditions have to be changed. As a result, the bounding process appears in a "black-box" manner for the analyst/designer whose only intervention consists in defining the quantity of interest. Furthermore, the non-intrusive technique enables one to easily tackle pointwise quantities by using Green's functions. Several numerical tests in two-dimensional and three-dimensional clearly illustrate the interest and efficiency of the proposed method.

In summary, this work demonstrates that reliable local error bounds can be obtained at reasonable cost for linear evolution problems, a fact which was not really accepted by the scientific community until now. It should be mentioned that the goal-oriented error estimation method proposed here does not use the orthogonality properties of the finite element solutions. Therefore, it could conceivably be applied to problems solved by approximation methods

other than the FEM; it could moreover be extended to other linear parabolic problems.

References

[1] I. Babuška, W.C. Rheinboldt, A posteriori error estimates for the finite element method, Int. J. Numer. Methods Eng. 12 (1978) 1597.

[2] P. Ladevèze, D. Leguillon, Error estimate procedure in the finite element method and application, SIAM J. Numer. Anal. 20 (3) (1983) 485–509.

[3] O.C. Zienkiewicz, J.Z. Zhu, A simple error estimator and adaptative procedure for practical engineering analysis, Int. J. Numer. Methods Eng. 24 (1987) 337–357.

[4] M. Paraschivoiu, J. Peraire, A.T. Patera, A posteriori finite element bounds for linear functional outputs of elliptic partial differential equations, Comput. Methods Appl. Mech. Eng. 150 (1997) 289–312.

[5] S. Prudhomme, J.T. Oden, On goal-oriented error estimation for elliptic problems: application to the control of pointwise errors, Comput. Methods Appl. Mech. Eng. 176 (1999) 313–331.

[6] P. Ladevèze, P. Rougeot, P. Blanchard, J.P. Moreau, Local error estimators for finite element linear analysis, Comput. Methods Appl. Mech. Eng. 176 (1999) 231–246.

[7] E. Stein, S. Ohmnimus, E. Walhorn, Local error estimates of fem for displacements and stresses in linear elasticity by solving local Neumann problems, Int. J. Numer. Methods Eng. 52 (2001) 727–746.

[8] N. Parès, J. Bonet, A. Huerta, J. Peraire, The computation of bounds for linear-functional outputs of weak solutions to the two-dimensional elasticity equations, Comput. Methods Appl. Mech. Eng. 195 (4–6) (2006) 406–429.

[9] K. Eriksson, D. Estep, P. Hansbo, C. Johnson, Introduction to adaptive methods for partial differential equations, in: A. Isereles (Ed.), Acta Numerica, Cambridge University Press, Cambridge, 1995, pp. 105–159.

[10] R. Rannacher, F.T. Suttmeier, A posteriori error control and mesh adaptation for finite element models in elasticity and elasto-plasticity, in: P. Ladevèze, J.T. Oden (Eds.), Advances in Adaptative Computational Method in Mechanics, Elsevier, Amsterdam, 1998, pp. 275–292.

[11] L. Chamoin, P. Ladevèze, Bounds on history-dependent or independent local quantities in viscoelasticity problems solved by approximate methods, Int. J. Numer. Methods Eng. 71 (12) (2007) 1387–1411.

[12] P. Ladevèze, Upper error bounds on calculated outputs of interest for linear and nonlinear structural problems, C. R. Acad. des Sci. Mec. Paris 334 (2006) 399–407.

[13] L. Chamoin, P. Ladevèze, A non-intrusive method for the calculation of strict and efficient bounds of calculated outputs of interest in linear viscoelasticity problems, Comput. Methods Appl. Mech. Eng. 197 (9–12) (2008) 994–1014.

[14] T. Strouboulis, I. Babuška, E. Copps, The design and analysis of the generalized finite element method, Comput. Methods Appl. Mech. Eng. 181 (2000) 43–69.

[15] P. Ladevèze, N. Moës, A new a posteriori error estimation for nonlinear time-dependent finite element analysis, Comput. Methods Appl. Mech. Eng. 157 (1998) 45–68.

[16] P. Ladevèze, J.-P. Pelle, Mastering Calculations in Linear and Nonlinear Mechanics, Springer, NY, 2004.

[17] R. Becker, R. Rannacher, An optimal control approach to shape a posteriori error estimation in finite element methods, in: A. Isereles (Ed.), Acta Numerica, vol. 10, Cambridge University Press, Cambridge, 2001, pp. 1–120.

[18] P. Ladevèze, Strict upper error bounds for calculated outputs of interest in computational structural mechanics, Comput. Mech. 42 (2) (2008) 271–286.

[19] R.D. Mindlin, Force at a point in the interior of a semi-infinite solid, J. Phys. 7 (1936) 195–202.

[20] R. Courant, D. Hilbert, Methods of Mathematical Physics, Interscience, New York, 1953.

[21] I.N Sneddon, R. Hill, Progress in Solid Mechanics, North-Holland, Amsterdam, 1964.